AFRL-ML-WP-TP-2007-509

FEMTOSECOND LASER THRESHOLD AND NONLINEAR CHARACTERIZATION IN BULK TRANSPARENT SiC MATERIALS (PREPRINT)

Chris Brewer and Shane Juhl

Hardened Materials Branch
Survivability and Sensor Materials Division

AUGUST 2007

Approved for public release; distribution unlimited.
See additional restrictions described on inside pages

STINFO COPY

AIR FORCE RESEARCH LABORATORY
MATERIALS AND MANUFACTURING DIRECTORATE
WRIGHT-PATTERSON AIR FORCE BASE, OH 45433-7750
AIR FORCE MATERIEL COMMAND
UNITED STATES AIR FORCE

NOTICE AND SIGNATURE PAGE

Using Government drawings, specifications, or other data included in this document for any purpose other than Government procurement does not in any way obligate the U.S. Government. The fact that the Government formulated or supplied the drawings, specifications, or other data does not license the holder or any other person or corporation; or convey any rights or permission to manufacture, use, or sell any patented invention that may relate to them.

This report was cleared for public release by the Air Force Research Laboratory Wright Site (AFRL/WS) Public Affairs Office and is available to the general public, including foreign nationals. Copies may be obtained from the Defense Technical Information Center (DTIC) (http://www.dtic.mil).

AFRL-ML-WP-TP-2007-509 HAS BEEN REVIEWED AND IS APPROVED FOR PUBLICATION IN ACCORDANCE WITH ASSIGNED DISTRIBUTION STATEMENT.

*//Signature//

CHRISTOPHER D. BREWER, Ph.D.
Direction Mgr, Space Systems Hardening
Exploratory Development
Hardened Materials Branch

//Signature//

MARK S. FORTE, Acting Chief
Hardened Materials Branch
Survivability and Sensor Materials Division

//Signature//

TIM J. SCHUMACHER, Chief
Survivability and Sensor Materials Division

This report is published in the interest of scientific and technical information exchange, and its publication does not constitute the Government's approval or disapproval of its ideas or findings.

*Disseminated copies will show "//Signature//" stamped or typed above the signature blocks.

REPORT DOCUMENTATION PAGE

Form Approved
OMB No. 0704-0188

The public reporting burden for this collection of information is estimated to average 1 hour per response, including the time for reviewing instructions, searching existing data sources, searching existing data sources, gathering and maintaining the data needed, and completing and reviewing the collection of information. Send comments regarding this burden estimate or any other aspect of this collection of information, including suggestions for reducing this burden, to Department of Defense, Washington Headquarters Services, Directorate for Information Operations and Reports (0704-0188), 1215 Jefferson Davis Highway, Suite 1204, Arlington, VA 22202-4302. Respondents should be aware that notwithstanding any other provision of law, no person shall be subject to any penalty for failing to comply with a collection of information if it does not display a currently valid OMB control number. **PLEASE DO NOT RETURN YOUR FORM TO THE ABOVE ADDRESS.**

1. REPORT DATE *(DD-MM-YY)*	2. REPORT TYPE	3. DATES COVERED *(From - To)*
August 2007	Journal Article Preprint	

4. TITLE AND SUBTITLE
FEMTOSECOND LASER THRESHOLD AND NONLINEAR CHARACTERIZATION IN BULK TRANSPARENT SiC MATERIALS (PREPRINT)

5a. CONTRACT NUMBER In-house
5b. GRANT NUMBER
5c. PROGRAM ELEMENT NUMBER 62102F

6. AUTHOR(S)
G. Logan DesAutels, Marc Finet, Scott Ristich, and Matt Whitaker (AT&T Government Solutions)
Chris Brewer and Shane Juhl (AFRL/MLPJA)
Peter Powers (University of Dayton)
Mark Walker (General Dynamics Information Technology, Inc.)

5d. PROJECT NUMBER 4348
5e. TASK NUMBER RG
5f. WORK UNIT NUMBER M08R1000

7. PERFORMING ORGANIZATION NAME(S) AND ADDRESS(ES)

AT&T Government Solutions
Dayton, OH 45433

Hardened Materials Branch (AFRL/MLPJA)
Survivability and Sensor Materials Division
Materials and Manufacturing Directorate
Wright-Patterson Air Force Base, OH 45433-7750
Air Force Materiel Command, United States Air Force

University of Dayton
Dayton, OH 45469

General Dynamics Information Technology, Inc.
5100 Springfield Pike, Suite 509
Dayton, OH 45431-1264

8. PERFORMING ORGANIZATION REPORT NUMBER
AFRL-ML-WP-TP-2007-509

9. SPONSORING/MONITORING AGENCY NAME(S) AND ADDRESS(ES)
Air Force Research Laboratory
Materials and Manufacturing Directorate
Wright-Patterson Air Force Base, OH 45433-7750
Air Force Materiel Command
United States Air Force

10. SPONSORING/MONITORING AGENCY ACRONYM(S)
AFRL/MLPJA

11. SPONSORING/MONITORING AGENCY REPORT NUMBER(S)
AFRL-ML-WP-TP-2007-509

12. DISTRIBUTION/AVAILABILITY STATEMENT
Approved for public release; distribution unlimited.

13. SUPPLEMENTARY NOTES
Journal article submitted to Optic Letters. The U.S. Government is joint author of this work and has the right to use, modify, reproduce, release, perform, display, or disclose the work. PAO Case Number: AFRL/WS 07-1679, 19 Jul 2007.

14. ABSTRACT
Semi-insulating and conducting SiC crystalline transparent substrates were studied after being processed by femtosecond laser radiation. Z-scan and damage threshold experiments were performed on both SiC bulk materials to determine each samples' nonlinear and threshold parameters. "Damage" in this text refers to an index of refraction modification as observed visually under an optical microscope. In addition, a study was performed to understand the damage threshold as a function of numerical aperture.

15. SUBJECT TERMS
Femtosecond, Numerical Aperture (NA), Silicon Carbide (SiC), Z-scan

16. SECURITY CLASSIFICATION OF:			17. LIMITATION OF ABSTRACT:	18. NUMBER OF PAGES	19a. NAME OF RESPONSIBLE PERSON (Monitor)
a. REPORT	b. ABSTRACT	c. THIS PAGE			Christopher D. Brewer
Unclassified	Unclassified	Unclassified	SAR	16	19b. TELEPHONE NUMBER *(Include Area Code)* N/A

Standard Form 298 (Rev. 8-98)
Prescribed by ANSI Std. Z39-18

Femtosecond Laser Threshold and Nonlinear Characterization in Bulk Transparent SiC Materials

G. Logan DesAutels[1], Chris Brewer[2], Peter Powers[3], Mark Walker[4], Shane Juhl[2], Marc Finet[1], Scott Ristich[1], Matt Whitaker[1]

[1]AT&T Government Solutions, Dayton, OH 45433
[2]Air Force Research Laboratory, Materials and Manufacturing Directorate, WPAFB, OH 45433
[3]University of Dayton, Dayton, OH 45469
[4]General Dynamics Information Tech., Dayton, OH 45431

Abstract – Semi-insulating and conducting SiC crystalline transparent substrates were studied after being processed by femtosecond laser radiation. Z-scan and damage threshold experiments were performed on both SiC bulk materials to determine each samples' nonlinear and threshold parameters. "Damage" in this text refers to an index of refraction modification as observed visually under an optical microscope. In addition, a study was performed to understand the damage threshold as a function of numerical aperture.

References and Links

1. Petite, Daguzan, Guizard, Martin, "Femtosecond History of Free Carriers in the Conduction Band of a Wide-Bandgap Oxide", Service de Recherche sur les Surfaces et l'Irradiation de la Matiere, Bat. 462, CE Saclay, 91191, Gif-sur-Yvette CEDEX, France.
2. Tien, Backus, Kapteyn, Murnane, Mourou, "Short-Pulse Laser Damage in Transparent Materials as a Function of Pulse Duration", University of Michigan, Physical Review Letters, Vol. 82, Number 19.
3. James Copper, Purdue Wide Band Gap Semiconductor Device Research Program, http://www.ecn.purdue.edu/WBG/Index.html, Purdue University College of Engineering.
4. Dong, Molian, "Femtosecond Pulsed Laser Ablation of 3C-SiC Thin Film on Silicon", Appl. Phys. A 77, 839-846 (2003).
5. Verdeyen, "Laser Electronics", Third Edition, Prentice Hall, Inc. 1995.
6. Lenzner, Kruger, Sartania, Cheng, "Femtosecond Optical Breakdown in Dielectrics", Physical Review Letters, Vol. 80, No. 18, May 1998
7. Ashcom, Schaffer, Mazur, "Numerical Aperture Dependence of Damage and White Light Generation from Femtosecond Laser Pulses in Bulk Fused Silica", Dept. of Physics, Harvard University; Dept. of Chemistry & Biochemistry, University of California.
8. Strelstov, Ranka, Geata, "Femtosecond Ultraviolet Autocorrelation Measurements Based on Two-Photon Conductivity in Fused Silica", Optics Letters, Vol. 23, No. 10, May 1998.
9. Shah, Tawney, Richardson, "Self-Focusing During Femtosecound Micromachining of Silicate Glasses", IEEE Journal of Quantum Electronics, Vol . 40, No. 1, Jan. 2004.
10. Evwaraye, Smith, Mitchel, "Determination of the Bandgap Offsets of the 4H-SiC/6H-SiC Heterojunction Using the Vanadium Donor (0/+) Level as a Reference", Appl. Phys. Lett. Vol. 67, No. 22, Nov. 1995.
11. Chapple, Staromlynka, Herman, McKay, "Single-Beam Z-scan: Measurement Techniques and Analysis", Journal of Nonlinear Optical Physics and Materials, Vol. 6, No. 3, Pgs 251-293, 1997.
12. Mansoor Sheik-Bahae, Ali A. Said, Tai-Huei,Wei, David J. Hagan, E. W. Van Stryland, "Sensitive Measurement of Optical Nonlinearities Using a Single Beam"; IEEE Journal of Quantum Electronics, Vol. 26, No. 4, April 1990, pg 760-769.
13. M. Yin, H. P. Li, S. H. Tang, W. Ji, "Determination of Nonlinear absorption and Refraction by Single Z-scan Method"; Appl. Phys. B, Vol. 70, pgs 587-591, 2000.
14. Yamane, Asahara, "Glasses for Photonics", Pg. 174.
15. Mao, Quere, Guizard, "Dynamics of Femtosecond Laser Interactions with Dielectrics", Appl. Phys. A 79, 1695-1709, 2004.

---

1. Introduction

Femtosecond (fs) lasers have become a very important tool for micromachining and fabrication of photonic devices. Their unique ability of inducing permanent index changes into just about any transparent material is due to fast focusing conditions, resulting in very high intensity causing nonlinear multi-photon absorption. Former research has theorized that the ultra-fast pulse is too short to interact at the molecular level, and instead interacts at the atomic electronic level [1]. Here the fs pulse displaces electrons permanently and/or causes lattice changes resulting in a modification to the index of refraction [2]. The modification to the index is localized to a very small volume depending on the NA and energy used. These index alterations can be on the surface or in most cases subsurface in bulk material.

SiC is an attractive alternative material for a variety of semiconductor devices where silicon (Si) lacks the environmental resistance that carbon furnishes when combined to Si. These areas where SiC devices can be used include high-power high-voltage switching applications, high temperature electronics, and avionics where the reduction of payload due to many wires

are needed to keep sensitive Si-based electronics away from extreme environments onboard aircraft [3]. However, SiC has issues related to micro-machining due to its problematic ability to resist almost any type of processing (etching). Examples of the common etching processes are: wet chemical etching, deep reactive ion etching (DRIE), and reactive ion etching (RIE) [4]. For these reasons, it is of some interest to study the laser processing and material characteristics of SiC to provide future alternative methods of micromachining this unique material.

Our method of morphing a circular beam into a high aspect ratio elliptical beam uses an anamorphic lens. The anamorphic lens transforms the ultrafast (UF) laser pulse from a 5.5mm round fluence distribution to a 2.5µm by 190µm line shape. The SiC samples were laser processed using an automated xyz stage in a direct write configuration. The samples were irradiated with a single laser pulse by use of a chopper wheel and high speed shutter combination. The fs laser pulse was generated using a Clark-MXR CPA-2010 laser system, with a wavelength of 780nm, a pulse width of 150-200fs, $M^2 = 1.55$ and a maximum energy of 1mJ/pulse. Typical pulse energies used in this work were in the 10µJ to 30µJ range.

In this work we report semi-insulating and conducting SiC bulk material linear and nonlinear optical properties, as well as bulk damage threshold (DT) measurements as a function of numerical aperture, NA, (under tight focusing conditions). The linear SiC material properties were measured using UV-Vis spectrometer, which determine the linear transmission and bandgap of the substrate. The 3rd order nonlinear properties are revealed using the Z-scan technique, which present the nonlinear absorption (β) and the nonlinear index of refraction (n_2). The laser processed portions of the samples were also investigated using optical microscope imagery, and atomic force microscopy (AFM). Finally, all experiments were first calibrated using a fused silica (FS) sample and compared to referenced experimental data to validate our results.

2. Experimental Setups

The DT and Z-scan experiments were completed using a single laser source split into multiple paths. Figure 1 below illustrates the experimental setups.

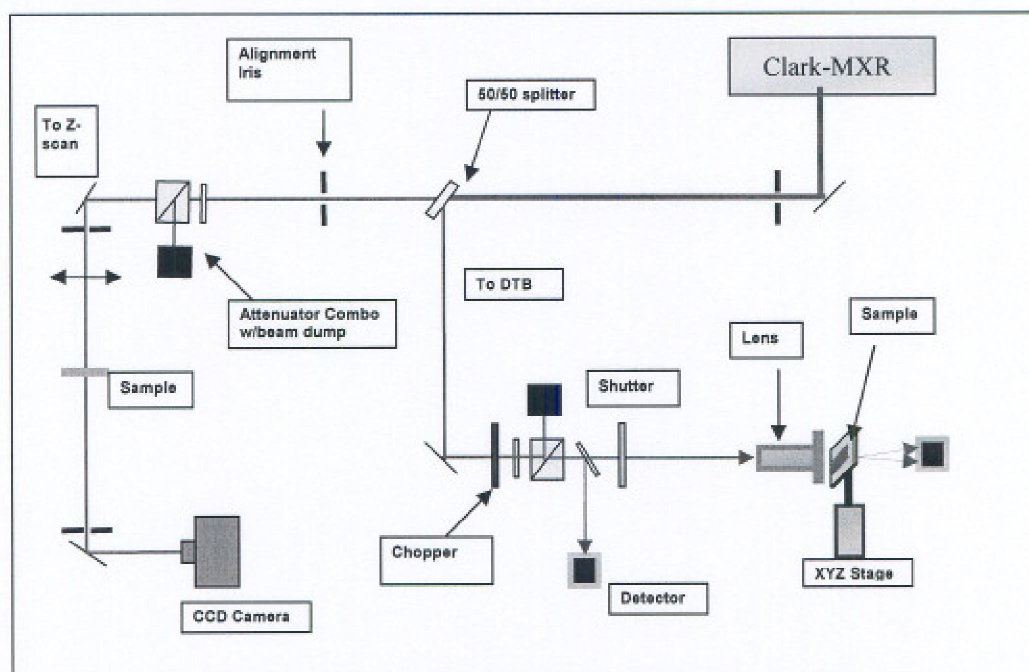

Figure 1 Setups for the damage threshold and Z-scan experiments.

Figure 1 gives the experimental setups for both the DT and Z-scan experiments. The Clark-MXR femtosecond laser system is split into multiple beam paths for different tests; a 100µJ portion of that is split for the DT and Z-scan studies. In each experiment line there is a polarizer beam splitter and ½ wave plate combo used to attenuate the beams. The Z-scan uses a 750mm lens to provide a large Rayleigh range, Z_R, and to keep the fluence below the damage threshold. The DT experiment uses the anamorphic lens to morph the 5.5mm circular beam into a 2.5µm x 190µm line distribution as described in the Introduction section.

The Z-scan line uses a CCD camera (DALSA 1M15) to sense the transmitted beam, and the closed aperture is added synthetically, via software image processing. The synthetic aperture types (round or other shapes), range of the Z-scan, and camera calibration are all set before each scan. The experiment uses a large CCD array (typically about twice the beam diameter after focus) and synthetic apertures have allowed ease in alignment of the beam down the Z-scan line. Typically, the open and closed apertures are set by the use of photodiode and iris combo, but that induces alignment sensitivity issues, whereas our Z-scan experiment uses a large array CCD the alignment is simple due to the synthetic apertures following a miss-aligned beam and for wedged samples. In addition, the software can record an average of beam profiles (intensity) at each Z-location, and then save those images for further analyses.

The DT line uses input and output photodiodes to measure the incident pulse energy verses the transmitted energy through the sample. Each photodiode is calibrated using a pyroelectric Joule meter (traceable to National Institute of Standards). The DT line also has a chopper wheel and a high speed shutter which together work automatically control the number of pulses to the sample. Finally, the sample is held on a xyz automatic stage controlled with ± 1μm accuracy. The entire illumination collection procedure is automated. This configuration, shown in Figure 1, allows for the Z-scan and DT experiments to run simultaneously, but the beams delivered at each experiment are separately characterized for completeness.

3. SiC Characteristics

The SiC samples tested are two types shown in Table 1 below.

Table 1: SiC sample characteristics for semi-insulating and conducting types. These values come from the vendor; semi-insulating SiC comes from Intrinsic Corp, and the conducting SiC comes from Cree Corp.

Sample	Conductivity	Orientation	Dopant	Concentration (cm^{-3})	Resistivity ($\Omega\cdot cm$)	Thickness (μm)	Face	N or P Type
SiC semi-insulating	Semi-insulating	c-plane, 6H 0° on axis	Undoped	~$1x10^{15}$	$3x10^{7}$	340	Si	---
SiC conducting	Conducting	c-plane, 6H 0° on axis	Nitrogen	~$2.5x10^{17}$	0.05	220	Si	N

Each sample in Table 1 was perpendicularly oriented on the c-plane with the vertically polarized circular and anamorphic beams. The nitrogen dopant amounts (~1 part per million) in the conducting sample are so small they can be ignored for this study. The thickness differences between the samples can also be ignored since these are surface studies. The lab/laser conditions are identical. Once the lenses were aligned and characterized each sample was simply inserted at the same location. The samples have the same dimensions therefore the identical sample mount/position was employed. The tests were run back to back so the laboratory environmental conditions were indistinguishable. Thus, the conductivity/resistivity is the only variable between the two samples.

4. Threshold Measurements

The damage threshold in this text refers to substrate modification observed under an optical microscope using transmission or reflection along with plots of transmission versus fluence measurements of the write pulse. The DT values are an important quantity to report for future laser processing of SiC bulk materials. The DT is measured in J/cm^2 and determines the minimum energy distribution to induce an observable change into the SiC material. The fluence distribution in the beam focus is well-designed as an elliptical and/or circular Gaussian with spot size along each principal axis given by [5],

$$w_{o\,x,y} = \frac{\lambda \cdot f_{x,y} \cdot M_{x,y}^{\;2}}{\pi \cdot w_z}, \qquad \text{Equation 1}$$

where f is the focal length, λ is the wavelength, w_z is the spot radius propagating from the laser, and is also known as the clear aperture (actual beam radius entering the lens). The M^2 is a measured quantity that is used to characterize the deviation from diffraction limited focusing (M^2 of 1 represents the diffraction limit, and real beams have $M^2 > 1$), and w_z is given below.

$$w_z = w_{ox,y} \cdot \sqrt{1+\left(\frac{Z}{Z_R}\right)^2}, \qquad \text{Equation 2}$$

where Z is the propagation distance from the laser source to the test bed, w_o is the beam spot size, and Z_R is the Rayleigh range. The peak fluence can be determined using

$$F_o = \frac{2 \cdot E}{\pi \cdot w_{ox} \cdot w_{oy}}, \qquad \text{Equation 3}$$

where E is the input energy. The above equations were used for each axis for the elliptical beam formed by the anamorphic lens system. Figure 2, Figure 3 and Table 2 give the damage threshold results for FS, semi-insulating and conducting SiC.

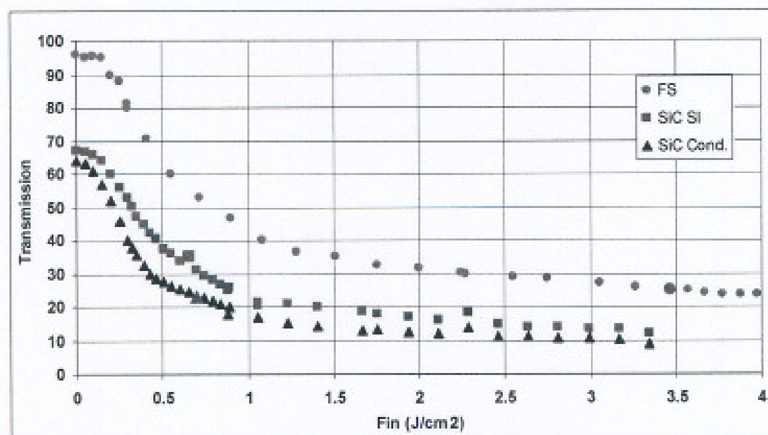

Figure 2 Damage threshold (DT) plot of SiC semi-insulating (SI), SiC conducting, and Fused Silica (FS). FS is our base-line sample, which is used to calibrate our DT experiments. FS has a DT that is well known to be ~3.0-4.0 J/cm^2 as referenced [6]. The larger red data points represent where the visible damage begins.

These DT results greatly depend on NA as shown in Schaffer-Mazur [7] for tight focusing conditions. In Figure 2, the DT data was recorded using a 125mm lens (NA = 0.022). To show the dependence of NA, as Schaffer-Mazur, we employed our anamorphic lens and repeated the DT plot in Figure 2; shown below in Figure 3.

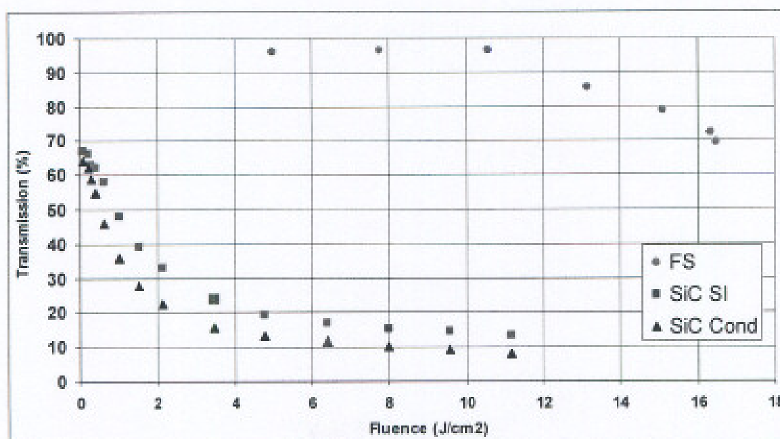

Figure 3 DT plots of SiC semi-insulating, SiC conducting, and FS as a function of fluence; the larger red data points represent where the visible damage begins.

The DT results are tabulated in Table 2 below.

Table 2: DT measured results for two lenses: 125mm focal and the anamorphic lens (High NA).

Sample	DT (J/cm^2)	High NA DT (J/cm^2)	Bandgap
FS	3.7	NA; ~20-40	9eV [8]
SiC semi-insulating	0.6	3.5	3.1eV [9,10]
SiC conducting	0.65	6.4	3.1eV [9,10]

As shown in Table 2 the use of a high NA increases the DT, as inspected under an optical microscope, by a factor of 6 to 10 times from the spherical 125mm lens. The FS sample did not reach a DT for the high NA experiment, and it is predicted that 100µJ (for a fluence of ~30 J/cm^2) or more is needed to create a 2.5µm X 190µm line on or below the surface. Thus, reported here are the damage thresholds in FS, SiC semi-insulating, and SiC conducting with a revealed dependence on NA.

5. Z-scan Study

The nonlinear properties, nonlinear index of refraction (n_2) and nonlinear absorption (β), of SiC semi-insulating and SiC conducting were also investigated. In calculating the nonlinear parameters two approximations are applied to reduce the computation speed and complexity. One is a thin sample approximation where the sample thickness >> Z_R, and the second is the weak nonlinear approximation that assumes the nonlinear process is small [11]. The calculated n_2 data is done using the peak to valley of the closed aperture trend defined by [12]

$$n_2 = \frac{\Delta\Phi_o}{kL} \cdot \frac{1}{I_o}, \quad \text{Equation 4}$$

where $\Delta\Phi_o$ is the on-axis phase shift at the focus, k is the wave number, L is the length of the sample and I(z,E) is the intensity as a function of z-position and energy for a $Sech^2$ pulse given by [12]

$$I(z,E) = \frac{2E \cdot \ln\left(1+\sqrt{2}\right)}{\Delta t \cdot \pi \cdot w_o^{\;2}}, \quad \text{Equation 5}$$

where Δt is the pulse width, w_x and w_y are the spot radii of the beam in x and y directions. As stated above, $\Delta\Phi_o$ is the on-axis phase shift, ΔΦ, which can be experimentally determined by examining the peak-valley transmission change in the closed aperture case using [12]

$$\left|\Delta\Phi_o\right| = \frac{\Delta T_{pv}}{(0.406)(1-S)^{0.25}}, \quad \text{Equation 6}$$

where S is the linear transmittance aperture (S-Parameter) and defined by [12]

$$S = 1 - \exp\left(-2\frac{r_a^{\;2}}{w_a^{\;2}}\right). \quad \text{Equation 7}$$

Here, r_a is the radius of the closed aperture and w_a is the radius of the laser beam at the location of the closed aperture. Equation 4 can then be used to recover the n_2 value of the sample under test.

We will not go into much detail with the fit data simply to keep this paper simplified, rather we direct the reader to reference [13], which describes precisely how to apply the theory and equations to any mathematical software such as Mathcad, Matlab, etc. The normalized open aperture signal is fitted to [13]

$$T_x(z,\beta,E) := \frac{1}{2\cdot q_o(z,\beta,E)}\cdot\int_{-\infty}^{\infty} \ln\left(1 + q_o(z,\beta,E)\cdot \operatorname{sech}(x)^2\right) dx \quad \text{, Equation 8}$$

where q_o is defined by [13]

$$q_o(z,\beta,E) := \beta\cdot I(z,E)\cdot L \quad \text{, Equation 9}$$

This work utilizes the open and closed fits to average the noise in the data. The peak-valley of the closed data fit is used to calculate the on-axis phase shift.

For the FS and SiC data a closed aperture of 0.55mm, and open aperture of 5mm, repetition rate of 41Hz (with assistance from a chopper wheel), an S-parameter set to 15%, and energy ranging from 2μJ to 3uJ. Multiple energies were used to ensure in consistent nonlinear measurements. The beam was characterized, before the experiments, by performing M^2, measuring the pulse width (using a Clark-MXR AC 150 Auto-correlator), and profiling the beam. The beam was profiled with and without the sample to properly calculate the S-Parameter (shown in Equation 7). The Z-scan data is shown as raw data with open and closed aperture data fits, which provide the n_2 and β results. The following figures confirm the Z-scan results.

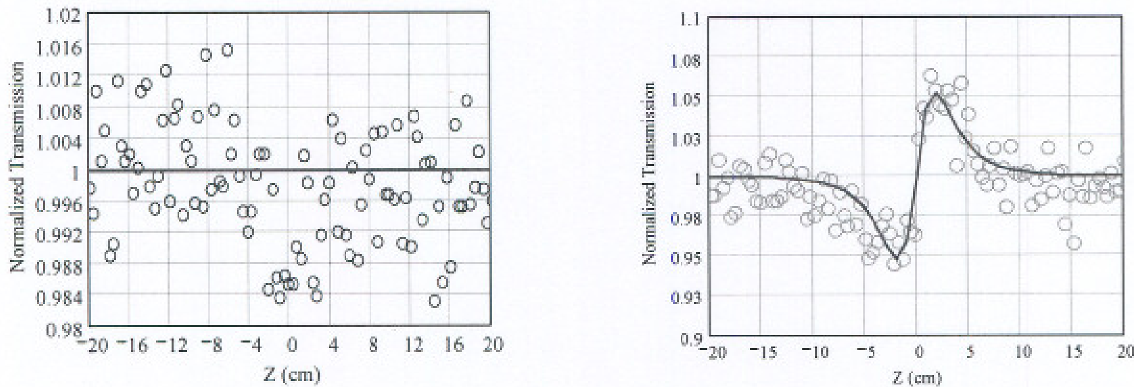

Figure 4 On the left is the normalized transmission for the open aperture and on the right is the normalized transmission for the closed aperture both for a fused silica reference sample. The parameters used for this sample were energy of 2μJ, a 750mm lens, and a 5.1mm entrance aperture.

From the data fits in Figure 4 results in a β = 0 cm/GW (Giga-Watts), and $n_2 = 2.6 \times 10^{-7}$ cm^2/GW. Referenced FS Z-scan results show similar n_2 values of 2.5×10^{-7} cm^2/GW [14], but published β values were not located primarily due to fact that FS has little or no nonlinear absorption (from large bandgap). Since the FS n_2 experimental result is in good agreement with the published values the Z-scan experiment is in good working order and is ready to test the SiC samples. The SiC samples were tested and the results are given in the figures below.

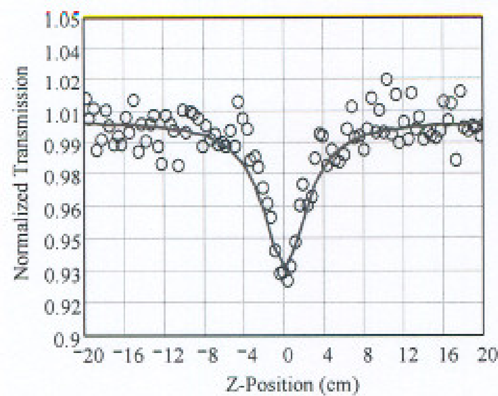

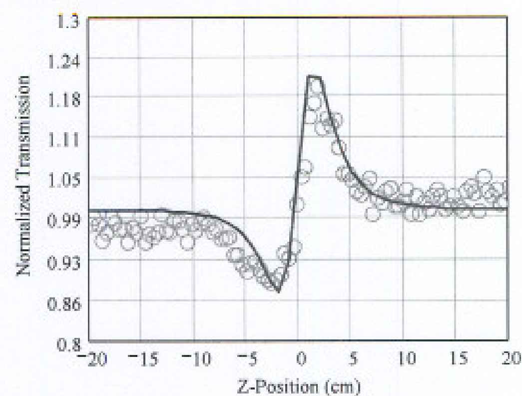

Figure 5 On the left is the normalized transmission for the open aperture and on the right is the normalized transmission for the closed aperture both for the SiC semi-insulating sample. The parameters used for this sample were energy of 3μJ, a 750mm lens, and a 5.1mm entrance aperture.

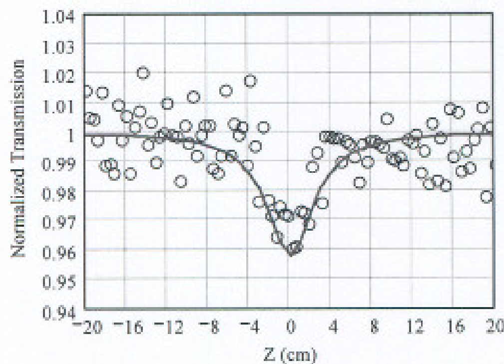

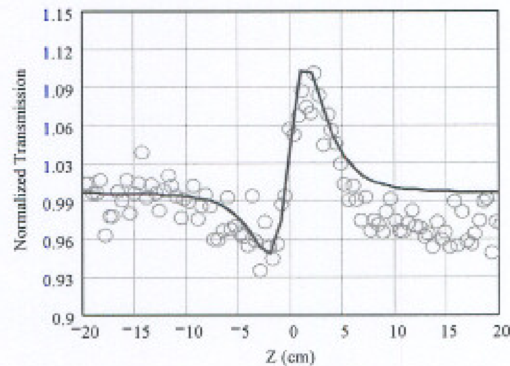

Figure 6 On the left is the normalized transmission for the open aperture and on the right is the normalized transmission for the closed aperture both for the SiC conducting sample. The parameters used for this sample were energy of 3μJ, a 750mm lens, and a 5.1mm entrance aperture.

The results for the SiC Z-scans are found in Table 3 along with the FS findings.

Table 3: DT measured results for two lenses: 125mm focal and the anamorphic lens (High NA).

Sample	Energy (μJ)	β (cm/GW)	n_2 (cm^2/GW)
FS	2	0	2.6×10^{-7}
SiC semi-insulating	2	0.072	5.1×10^{-6}
SiC conducting	2	0.048	4.1×10^{-6}
FS	3	0	2.4×10^{-7}
SiC semi-insulating	3	0.056	4.4×10^{-6}
SiC conducting	3	0.056	4.0×10^{-6}
FS Average	---	0	2.5×10^{-7}
SiC semi-insulating Ave.	---	0.064	4.75×10^{-6}
SiC conducting Ave.	---	0.052	4.05×10^{-6}

From Table 3 the FS is for reference only, but the SiC data is of interest. The semi-insulating and conducting SiC nonlinear properties are relativity the same, which is not surprising since the dopant levels in the conducting sample are extremely small as stated earlier. The conductivity is electronic therefore it has no or little affect on the optical linear/nonlinear

interactions; only the SiC compound affects the absorption and index (linear and nonlinear), thus the nonlinear quantities are about the same.

6. UV-Vis Study

A UV-Vis study was carried out to understand the linear transmission and to confirm the provided bandgap information shown in Table 2. A Varian Cary 50 UV-Vis spectrometer was used to perform the experiment. It was setup to use a Xenon flash lamp and monochromatic optics to send a beam of varying wavelengths (300nm to 900nm) through the sample to measure its transmission. The results for each SiC sample are given in the figure below.

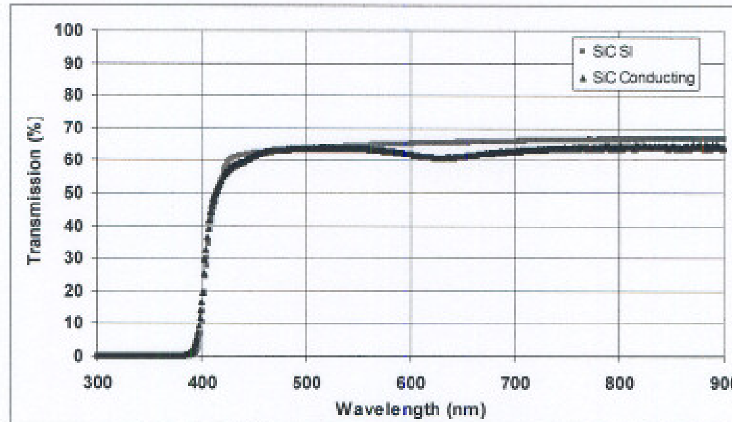

Figure 7 UV-Vis results on semi-insulating and conducting SiC.

From the UV-Vis results it demonstrate that both the semi-insulating and conducting SiC samples "turn on" at the same wavelength, 400nm. Equation 12 below relates the "turn on" wavelength of the SiC samples to the band gap in electron volts (eV) stated in Table 2.

$$\lambda = \frac{1239.8}{E(eV)}. \qquad \text{Equation 10}$$

Here, E is the energy with units of electron volts, λ is in units of nano-meters (nm), and Table 2 gives E = 3.1eV. Therefore, λ = 399.936 nm for both semi-insulating and conducting SiC, which is in agreement with the "turn on" wavelength in Figure 7. Furthermore, the conducting SiC sample has a dip centered at ~630nm that is consistent with multiple SiC conducting samples tested. The dip is may be due to the absorption of the Nitrogen dopant present in the conducting SiC sample. The transmissions are around 65% to 70% for each semi-insulating and conducting sample, which agrees with the DT results.

7. Sample Characterization

The high NA line distribution processed (processed lines) into the SiC semi-insulating and conducting samples were further analyzed using optical microscopy and Atomic Force Microscopy (AFM) to understand the morphology of the index modified structures. The processed lines are on or just below the surface (~5μm to10μm), and the modifications form a hill/valley above/below the surface depending on the type of SiC processed. The figures below illustrate this effect.

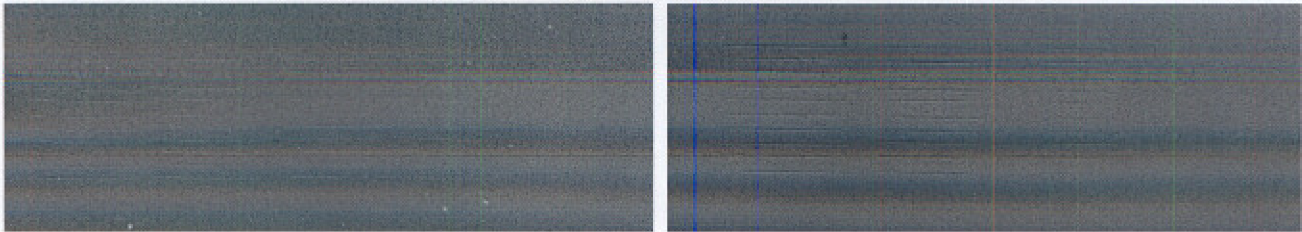

Figure 8 DT optical microscope results using Nomarski DIC and image processing for better viewing purposes for (left) semi-insulating SiC; (right) conducting SiC. Image processing was performed in order to better resolve the modified surface lines.

For these images, the optical microscope used is an Olympus upright digital BX51 microscope with Nomarski DIC capabilities that use high contrast prisms to produce increased contrast/resolution. This microscope also has measuring capabilities to $\pm$ 0.25μm or less, which is also traceable to NIST.

Here, the 2.5μm x 190μm *predicted* line spread is actually ~5.5μm wide x 210μm long for the semi-insulating SiC and ~3.3μm wide x 193μm long for the conducting SiC sample. The difference in the predicted primarily comes from the sample makeup and the sample being at the exact focus as foreseen. The line spread (for semi-insulating and conducting both) decreases in both axes as the fluence/energy is decreased until the point where no visible damage occurs. The semi-insulating SiC sample results in more columns of modified lines which are due to it having a lower threshold than the conducting SiC sample. The processed lines, on both SiC types, were analyzed using the Nomarski DIC mode on the optical microscope (set in reflection mode). The semi-insulating SiC processed lines are more optically opaque, which may be caused from bulges or hills that form in the surface as observed in other types of bulk transparent dielectric substrates. AFM imaging will give a more precise measurement of the line spread morphology.

Atomic Force Microscopy (AFM) was used in tapping mode to evaluate the topography of line distributions fabricated below the threshold. In addition to height images obtained from monitoring the cantilever oscillation amplitude during scanning, surface potential measurements can be obtained from monitoring the AFM cantilever response during an application of voltage, which gives us information on the electric field distribution. Figure 9 below shows some AFM results of a SiC semi-insulating sample with surface line modifications.

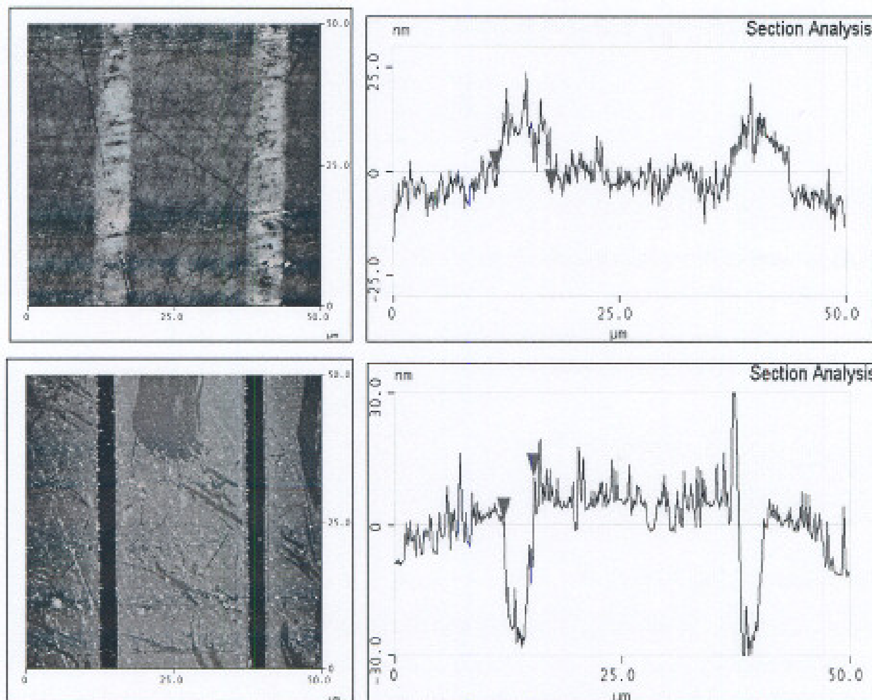

Figure 9 On the top shows AFM results of a 5.5μm wide and a 10nm raise surface modification on semi-insulating SiC material. On the bottom shows the conducting SiC sample AFM results of a 3.3μm wide and a 30nm trench surface modification.

The AFM results show a morphology of the line processed structures as being 3-5μm in width and about a 10-30nm hill or valley. The semi-insulating SiC sample forms lines protruding bulges that are raised by ~10nm and have a width of ~5.5μm. The conducting SiC sample forms line trenches that are ~30nm deep and have a width of ~3.3μm. The AFM concludes that the semi-insulating SiC surface modification by these line spreads creates a hill in the substrate surface, which may be due to a local subsurface restructuring has occurred or some other electronic trapping process [15] has forced the material to rise in the processed areas. Whereas, the conducting SiC sample forms trenches that may be due to surface structural damage caused by thermal breakdown of the molecular lattice to the inability for the crystal to dissipate heat, and/or oxidation and chemical reactions on the surface that give a different compound. The protruding lines in the semi-insulating sample also caused a broader line width instead of the predicted 2.5-3μm, and the valleys formed in the conducting samples create a sharper edge that results in a closer agreement to the predicted value. In any case, there is a morphology difference in the femtosecond laser processing of SiC between semi-insulating and conducting types.

8. Conclusion

In this work we report important linear, nonlinear and femtosecond laser processing threshold properties that are useful to optical and material scientific communities. We concluded that there are only two observable differences between the two SiC types (even the samples visual appearance is similar), which are the UV-Vis absorption at ~630nm and the morphology after being femtosecond laser processed. The linear, nonlinear, and DT properties remain familiar to one another. The values of all the measured parameters vary within 20% of each other except for the high NA DT values which gives a 45% difference between semi-insulating and conducting types. Special thanks is given to AFRL personal Don Dorsey, Tom Kensky for providing the SiC samples, and to Angela Campbell for assisting with AFM results.